ISSN 2347-3487

Modification of Pb-Sb eutectic bearing-solder alloys with bismuth additions rapidly solidified from melt

Rizk Mostafa Shalaby[1,*], Bilal W. Mahdi [1, 2], Abu-Bakr El-Bediwi[1], and Mustafa Kamal[1]
[1] Metal Physics Lab. Physics Department Faculty of Science, Mansoura University, Mansoura, Egypt
[2] On leave, M.Sc. student, Iraq

Abstract

In this work, various amounts of Bi element have been added to the eutectic Pb-Sb to form bearing- solder materials. The Pb-Sb eutectic has been produced by rapid solidification using melt spinning technique with various amounts of Bi have been added to it, in the ratio 1, 2 , 3, 4, and 5 wt.%. Scanning electron microscopy (SEM), X- ray diffraction (XRD) analysis and differential scanning calorimetry (DSC) have been carried out. Microhardness measurements were also carried out using Vicker's hardness technique. The results showed that, the ternary alloys up to 4 wt.% Bi have properties superior to binary eutectic material. Bismuth up to 4wt. % increases the Young's modulus, Vicker's hardness and decreases the electrical resistivity, internal friction and melting point. The ternary Pb-13.1Sb-4Bi solder alloy has a lower melting point about 237.87 ˚C. Also, the results show that formation of Bi phase developed the mechanical properties and Vicker's hardness due to addition of Bi element. The addition of Bi refines the crystal size of Sn in case of melt spun alloys as seen in scanning electron micrographs and X-ray diffraction.

Keywords

Bismuth addition; structural; mechanical properties; thermal analysis; electrical properties.

Council for Innovative Research
Peer Review Research Publishing System
Journal: JOURNAL OF ADVANCES IN PHYSICS
Vol. 10, No. 1
www.cirjap.com, japeditor@gmail.com

ISSN 2347-3487

1. Introduction

Solidification is a critical stage in the processing of metallic materials, which has a strong influence on the material properties of the final metallic products, so interest in rapidly solidified metal has increased dramatically in the past few years. The application of rapid solidification technology (RST) leads to refinement, increased homogeneity distribution of very small second phase particles and increased solid solubility have a decisive influence on the behavior of the metallic materials. Varich and Yakumin [1] reported terminal solid solubility extension in Pb binary alloys up to 5.5 at.% Sb using quenching technique. The lead base provides low cost, low melting point and ease in casting. Additions of antimony not only harden the alloy and make it more resistant to compressive impact and wear, but also lower the casting temperature and minimize contraction during freezing. About 70.8 % of the lead produced in the world goas into lead-acid storage batteries for aeronautical, automotive, and marine applications. Lead acid batteries contain lead –antimony alloy with minor additions of copper, arsenic, tin, selenium. The Pb-Sb alloy system was investigated by Borromee-Cautier et al [2] at -190 C. Metastable single phase alloy was obtained instead of equilibrium two-phase alloys. New phase found include a bcc Pb-Sb phase, a primitive cubic coordinated Pb-Sb phase. A series of lead –antimony alloys were quenched from the melt by the splat cooling technique were reported by Ramachandraro et al in (1970) [3]. The resultant foils were studied by x-ray and electron microscopic techniques. No new crystalline intermediate phases were detected. However, there was evidence for amorphous solidification in the alloy containing 48 % Sb. Rapid solidification effects in Pb-Sb eutectic alloys had studied by M.Kamal and R.M.Shalaby [4]. They are concluded that the microstructural features of the alloys showed the presence of antimony particles at grain boundaries and within grains of the lead matrix. The study suggests that the quenching from melt induced increases in hardness and delaying the fracture. Also, electrical transport is observed that it is sensitive to the structure of the quenched ribbons. Lead-antimony alloys are very important materials in industry for their use as die casting alloys, the manufacture of cable sheathing and battery grids and in manufacturing acidic accumulators. Some physical and structure properties of a series of Pb-Sb alloys containing different additives were studied [5]. The alloys of the Pb–Sb system form a single-eutectic phase diagram without chemical compounds [6]. To organize electrorefining of lead–antimony alloys in ionic media, it is necessary to know the thermodynamic characteristics of the process conditions, which are quite different for liquid alloys of the Pb–Sb system [7-11]. The Pb-Sb system is a simple eutectic one with two phases: liquid, face-centered cubic (Pb), and rhombohedral (Sb). Results of several constitutional experiments and thermodynamic calculations were published in the literature. Liquidus line was determined by Dean,[12] Blumenthal,[13] and Moser et al.[14] who used thermal analyses. The structure and growth characteristics in the melt quenched alloys of Pb-Sb system were reported by Kamal et al[15] They found that the amorphous phases were found in a limited composition range around a hypoeutectic composition. The laser treatment of the conventional battery grid alloys such as lead antimony was performed to improve mechanical properties, mechanical creep, and corrosion properties have been investigated by Dahotre et al [16] They found that creep tests conducted under the conditions of constant load (1 Kg) and temperature (25 OC) showed a large improvement in the creep resistance compared to that of the as receved lead alloys. Using Melt-spinning Technique with Calcium Addition on the Ternary Pb-Sb-Sn Alloys for Storage Battery Grids were reported by Kamal et al [17]. They found in terms of mechanical properties, the addition of calcium to the Pb-Sb-Sn ternary alloy causes the increase of the hardness. The effect of bismuth on transport and mechanical properties of binary Pb-Sb eutectic alloy was measured and compared with the transport and mechanical properties of the binary alloy. The results of this research study provide necessary data for the modelling of solder joint reliability. The objective of this study aims to investigate the effect of small additions of Bi on structure, transport and mechanical properties of eutectic Pb-Sb bearing-solder alloys rapidly solidified from melt.

2. Experimental techniques

The experimental techniques utilized have been described in details [18-21] and will be repeated here only briefly. High purity materials have been used for the preparation of metallic alloys. The raw materials were melted in a porcelain crucible in an electric furnace at temperature ranging from 700-1000 K The alloys under investigation were produced by a single roller type melt spinning technique using a copper wheel at speed of 30.4 ms-1. Ribbon samples about 0.5-1.0 cm in width and 100-120 mm in thickness. The structure of the quenched ribbons was investigated using X-ray diffraction analysis was done on a Shimadzu x-ray diffractometer (DX-30), using Cu kα radiation (λ=1.5406 Å) with Ni-filter at room temperature and scanning electron microscopy. Microhardness tests were conducted using a digital Vickers microhardness tester (model FM7) via Vickers diamond pyramid. Differential thermal analysis (DTA) was used to determine the melting temperature of the alloys using Shimadzu DTA-50 instrument operating in heating mode. The microstructure analysis was carried out on a scanning electron microscope (SEM) of type (JEOL JSM-6510LV, Japan) operate at 30 KV with high resolution 3 nm.

3. Results and discussions

3.1 X-ray diffraction study

X-ray diffraction method was used to determine the phases of the six bearing-solder alloys by using DX-30, Shimadzu, Japan. The peaks in x-ray diffraction pattern are directly related to the atomic distances. X-ray Diffraction (XRD): XRD is a powerful and routine technique for determining the crystal structure of crystalline materials [22-24]. By examining the diffraction pattern, one can identify the crystalline phase of the material. Small angle scattering is useful for evaluating the average interparticle distance while wide-angle diffraction is useful for refining the atomic structure of nanoclusters [25]. The widths of the diffraction lines are closely related to the size, size distribution, defects and strain in nanocrystals. As the size of the nanocrystals decreases, the line width is broadened due to loss of long range order relative to the bulk. Fig.1 (a-f) shows the x-ray diffraction pattern of spun Pb -Sb13.1-Bix (where x varying from 0 to 5 wt. %) ribbons rapidly

ISSN 2347-3487

quenched from melt. This technique is used to determine the degree of crystallinity, unit cell shapes, and lattice parameters. The x-ray diffraction results of the melt spun alloys showed several peaks as shown in Fig.1.The diffraction peaks were sharp and distinct. The pattern shows the existence of different kinds of phases, Pb-phase with cubic structure Sb-phase with rhombohedral (hex) structure, and Bi-phase with rhombohedral (hex) structure. The diffraction peaks of the Bi phase appears at 2θ= 45. The x-ray details and crystal size of all alloys are calculated and summarized in Table 1. It is shown that the crystal size of α-Pb is decreased with Bi composition from 35.3 nm at binary eutectic alloy to 34.5 nm at 1.0wt% bismuth. The crystalline size is determined from the XRD pattern by using Scherer's equation Dhkl=0.9λ/βhklcosθ, where Dhkl is the crystalline size, λ is the wavelength of Cu Kα =1.54056 Å, θ is the reflection angle and βhkl is the full width at half maximum (FWHM) [26].

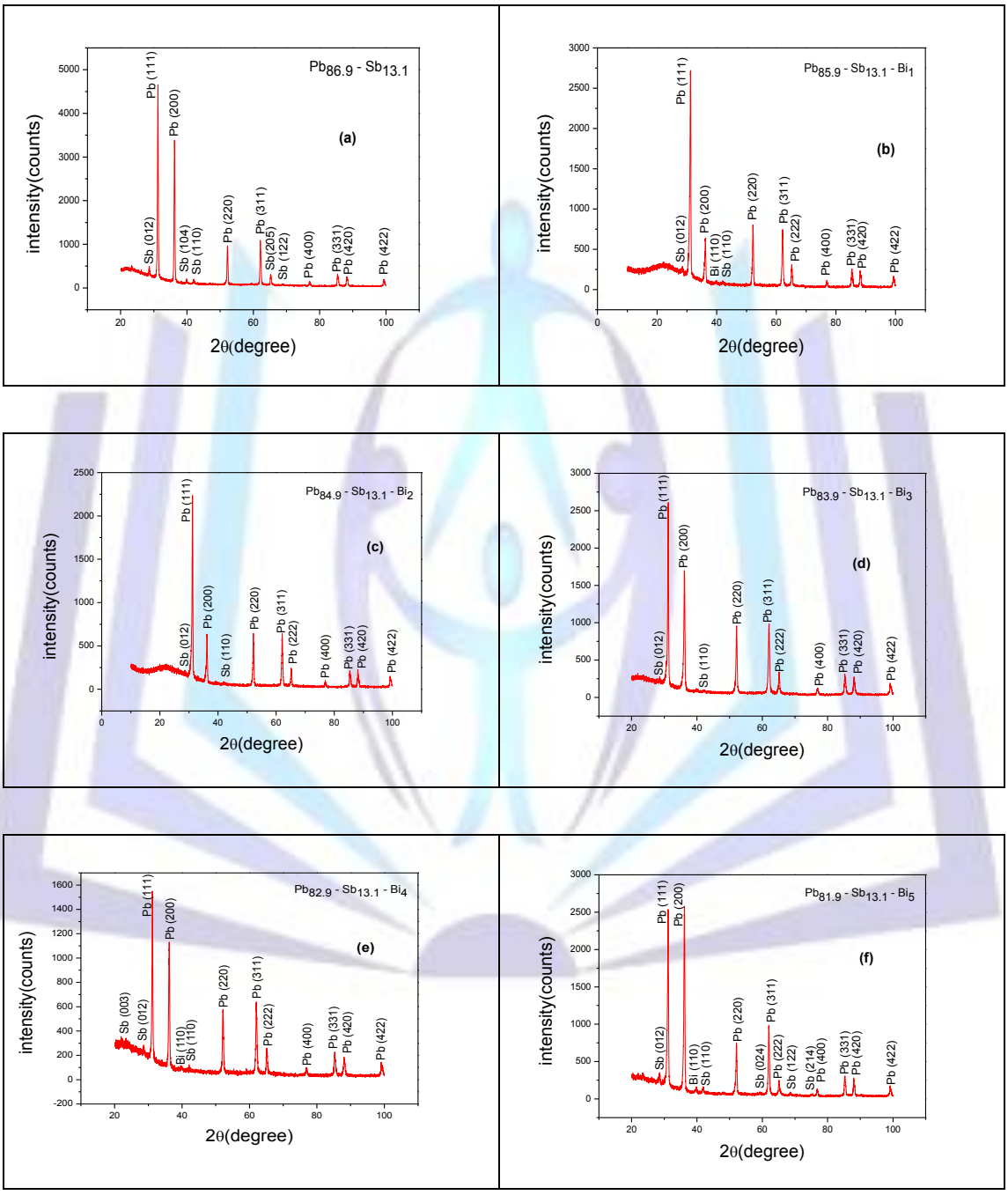

Fig. 1: X-ray diffraction patterns of Pb - Sb13.1 – Bix (x = 0, 1, 2, 3, 4 and 5 wt. %) melt spun alloys.

ISSN 2347-3487

Table 1: XRD details of Pb-Sb-Bi melt spun alloys

system wt%	a (Å) Cell	Volume ($Å^3$)	Density (g/cm^3)	No. of atoms per unit cells	Particle size (nm)
$Pb_{86.9}$ – $Sb_{13.1}$	4.9575	121.84	7.50	2.81	35.3
$Pb_{85.9}$ - $Sb_{13.1}$ - Bi_1	4.9592	121.97	8.57	3.21	34.5
$Pb_{84.9}$ - $Sb_{13.1}$ - Bi_2	4.9606	122.07	8.00	3.00	36.1
$Pb_{83.9}$ - $Sb_{13.1}$ - Bi_3	4.9624	122.20	8.00	3.00	37.3
$Pb_{82.9}$ - $Sb_{13.1}$- Bi_4	4.9640	122.32	8.54	3.21	38.7
$Pb_{81.9}$ - $Sb_{13.1}$ - Bi_5	4.9611	122.10	6.52	2.44	36.7

3.2 Microstructure of Pb-Sb-Bi bearing-solder alloys:

Fig. 2 shows the scanning electron micrographs of Pb-13.1Sb-Bix (x = 0, 1, 2, 3, 4 and 5 wt. %) melt spun alloys. From Fig.1a, it can be seen that there are two kinds of Pb-Sb phases in alloy, the dark-color particles and the light –color particles. From Fig.1b-f there are three kinds of Pb-Sb-Bi phases in alloy, the dark-color particles, the light –color particles and gray color particles. The particles have uniform particle size around 30-40 nm as indicated in XRD. The microstructural refinement can be clearly seen in melt spun alloys in all micrographs are shown in Fig.1(b-f) after addition of bismuth.

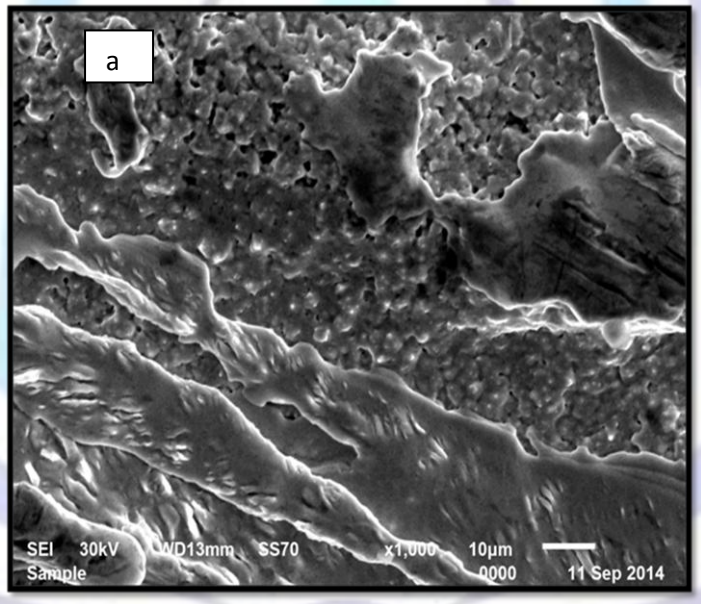

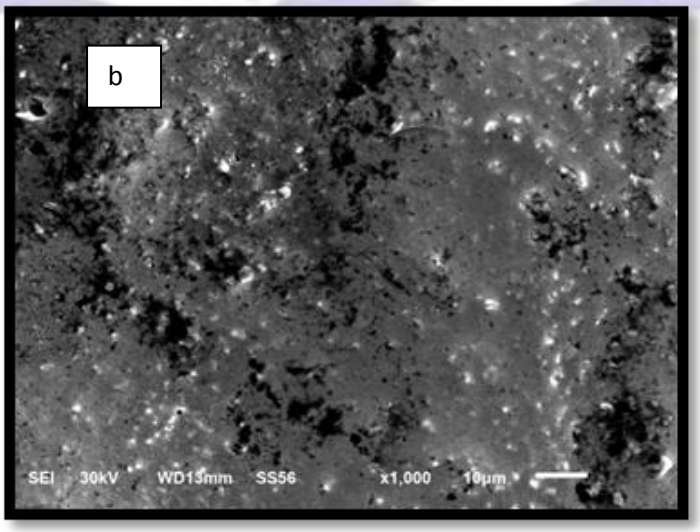

ISSN 2347-3487

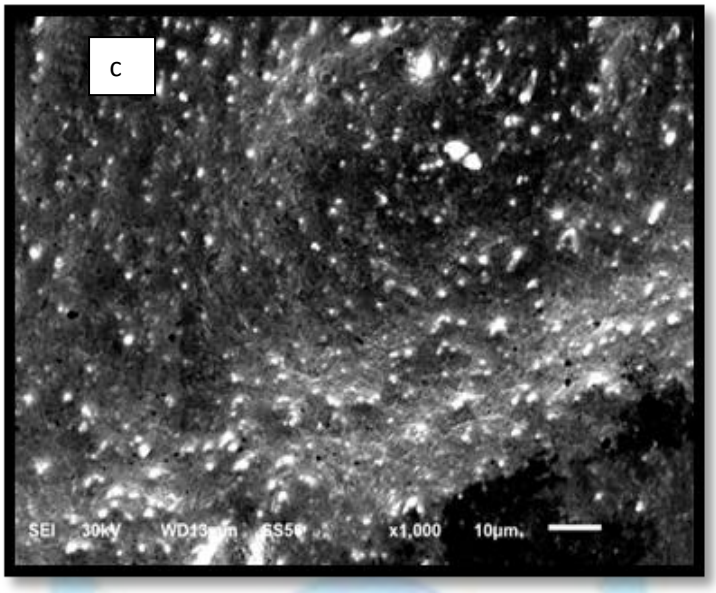

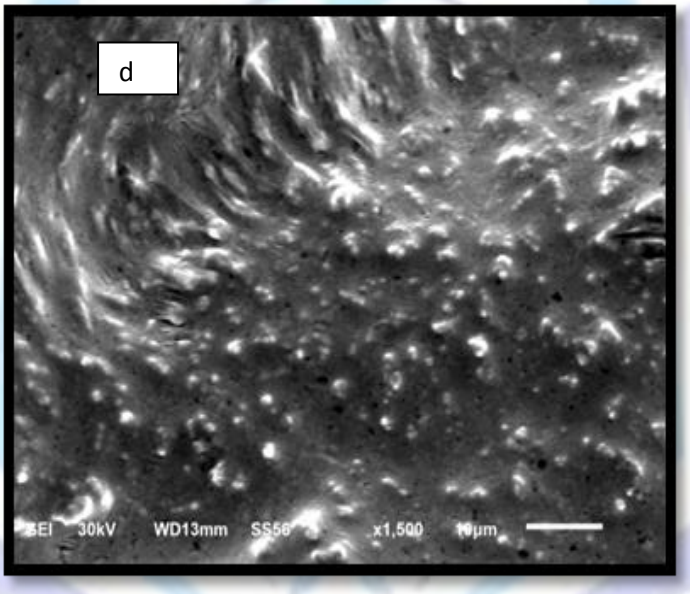

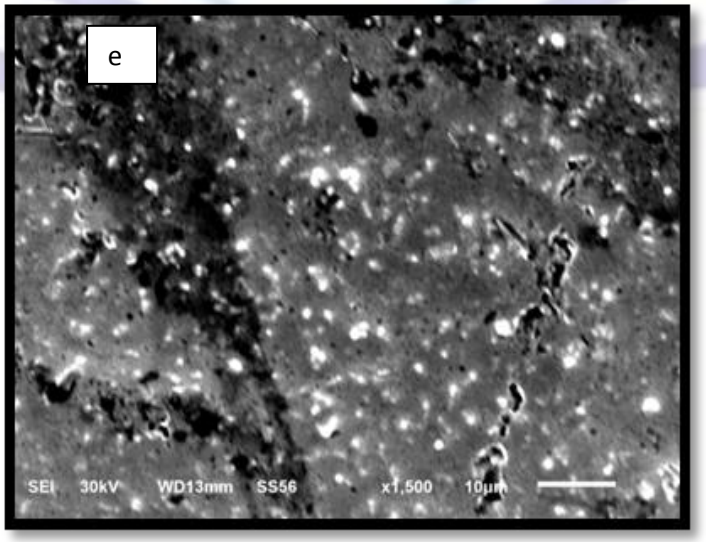

ISSN 2347-3487

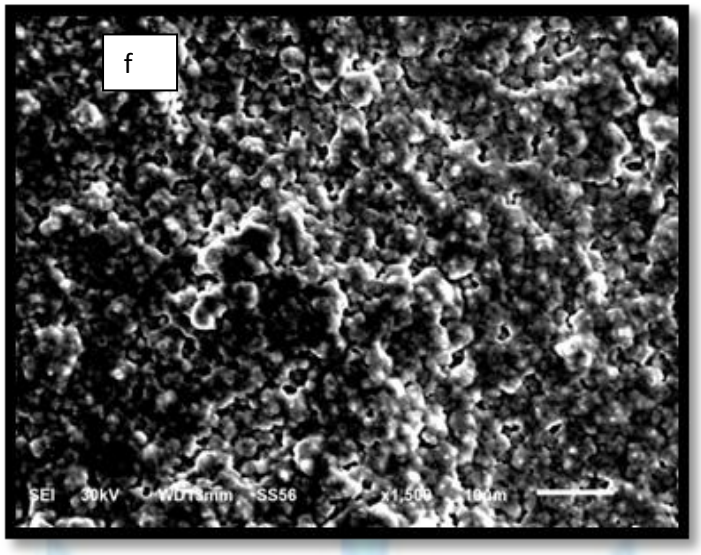

Fig. (2): SEM images for Pb – Sb13.1 – Bix (x= 0,1, 2, 3, 4 and 5 wt.%)

3.3 Thermal analysis:

The melting temperature is a critical characteristic because it determines the maximum operating temperature of the system and the minimum processing temperature of the system and the minimum processing temperature which its components must survive. Melting temperature is a vital thermal property and has a strong influence on surface mount technology (SMT) field. A promising solder alloy should have a low melting temperature zone [27]. Huang [28] found that the onset point in the DSC heating curve represents the solidus temperature and that the peak point shows the liquids temperature. Fig 3 (a-e) shows the DSC curves for Pb86.9-x-Sb13.1-Bix (where X were varying from 0 to 5 wt. %) melt spun alloys. Zu et al. [29] suggested that structural changes take place to some extent in molten alloys as a function of temperature, which have been confirmed by the corresponding calorific peak in a differential scanning calorimeter. So in this section, it is noted that further work is needed to probe the concrete change of structures with the help of a differential scanning calorimeter. Specimens approximately 7 mg in mass were cut from the melt-spun ribbons and were submitted to heating from room temperature to about 400 ˚C at rates of 10 K.min-1 in a SDTQ600 differential scanning calorimeter DSC. A typical output is depicted in Fig. 3 (a-e) the results of the melting temperature, enthalpy, entropy change and the average specific heat are tabulated in Table (2). As we see from table (2) melting point for all quenched ribbons is around (225-250) ˚C and there is a noticeable magnificent decrease in entropy change and specific heat as we add bismuth with minimum value at 3 wt. % of bismuth addition.

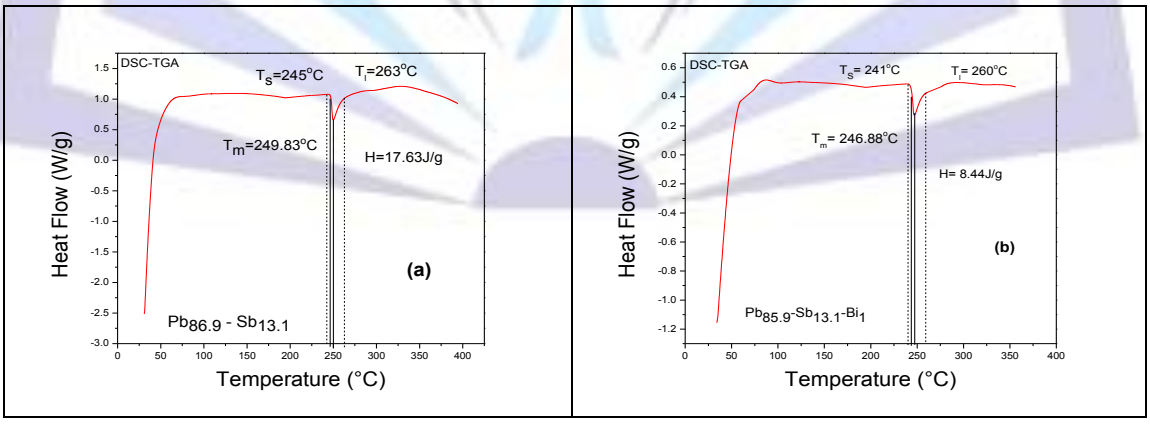

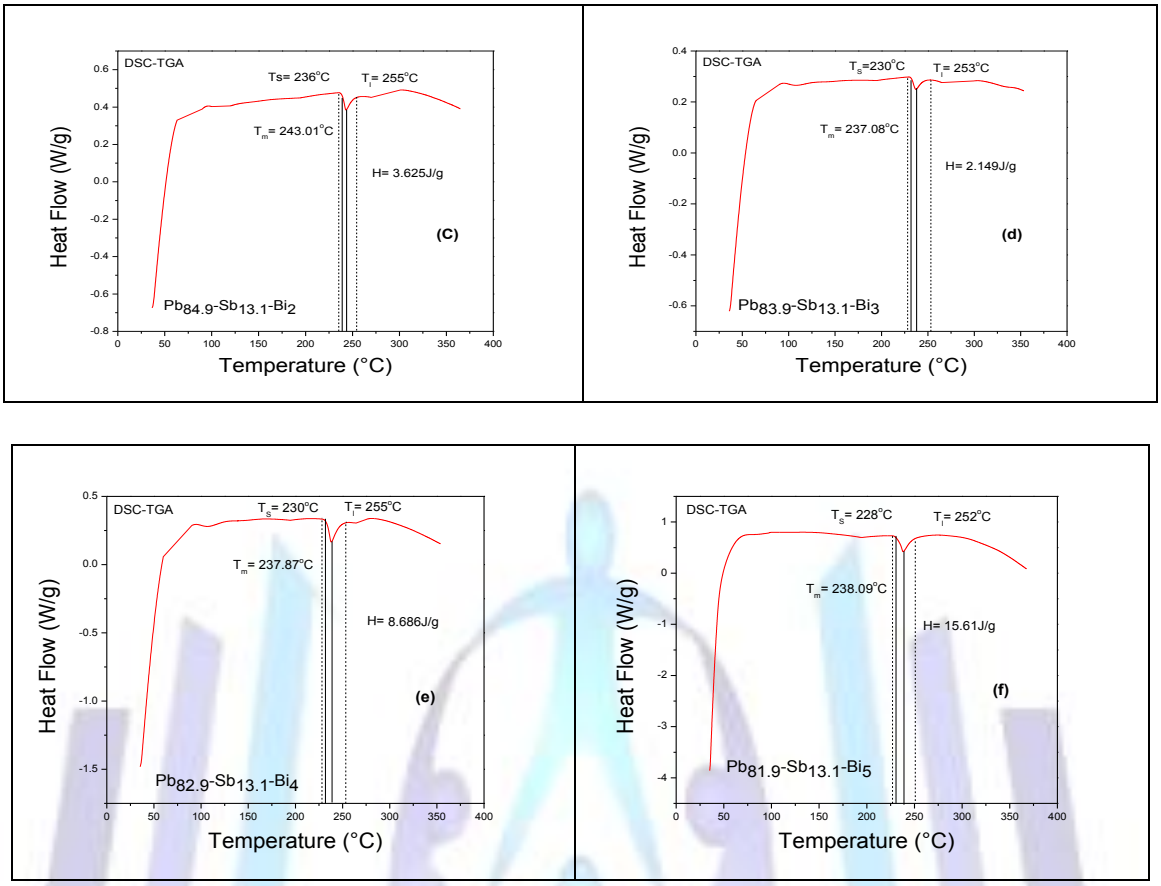

Fig.3 : DSC curves for Pb – Sb13.1 – Bix (x= 0,1, 2, 3, 4 and 5 wt.%) melt spun alloys.

Table (2): Thermal analysis of Pb –13.1 Sb – Bix (x= 0,1, 2, 3, 4 and 5 wt.%) melt spun alloys

System	T_s (K)	T_m (K)	T_l (K)	Pasty range (K)	Enthalpy (j/g)	Specific heat (j/g.K)	Entropy change (j/g.K)*10^{-2}
$Pb_{86.9}$ – $Sb_{13.1}$	518	522.83	536	0	17.63	0.979	3.35
$Pb_{85.9}$ - $Sb_{13.1}$ - Bi_1	514	519.88	533	19	8.441	0.444	1.61
$Pb_{84.9}$ - $Sb_{13.1}$ - Bi_2	509	516.01	528	19	3.625	0.191	0.69
$Pb_{83.9}$ - $Sb_{13.1}$ - Bi_3	503	510.08	526	23	2.149	0.093	0.41
$Pb_{82.9}$ - $Sb_{13.1}$ - Bi_4	503	510.87	528	25	8.686	0.347	1.69
$Pb_{81.9}$ - $Sb_{13.1}$ - Bi_5	501	511.09	525	24	15.61	0.650	3.04

3.4 Mechanical properties

The dynamic resonance method has a definite advantage over static method of measuring elastic moduli because the low-level alternating stress does not inflate an elastic processes such as creep or elastic hysteresis [30]. The elastic moduli obtained with the resonance method give information about elastic compliances along the long axis of the melt-spun ribbons. In an elastically isotropic body such as a well prepared polycrystalline quenched ribbons, the elastic moduli are identical in any direction. Elastic moduli can be obtained from frequency fo, at which peak damping occurs, according to:

$$E = \frac{38.32\rho l^4 f_0^2}{t^2} \quad \ldots\ldots\ldots\ldots\ldots\ldots\ldots (1)$$

$$G = \frac{E}{2(1+\nu)} \quad \ldots\ldots\ldots\ldots\ldots\ldots\ldots\ldots (2)$$

ISSN 2347-3487

$$B = \frac{E}{3(1-2\nu)} \quad \ldots\ldots\ldots\ldots\ldots\ldots\ldots\ldots (3)$$

Where, E is elastic modulus (Young's modulus), ρ is ribbon density, l is vibrated part of ribbon, t is ribbon thickness, G is shear modulus, B is bulk modulus and v is Poisson's ratio. Fig (4) shows the Young's modulus of the melt quenched ribbons. It is evident that Young's modulus of eutectic Pb – Sb is increasing as the bismuth content increase. Young's modulus of eutectic Pb – Sb was 12.5 (Gpa) and with the addition of 4 wt. % of bismuth it was raised up to 17.3 (Gpa), or about 5% higher than the original value.

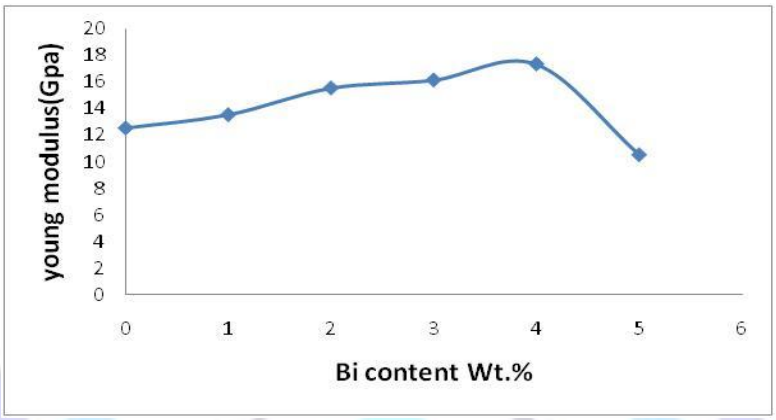

Fig. (4): Young's modulus Vs. Bi content

Ledbetter [31] and Gorecki [32] reported a theoretical basis for the experimental relationship between Young's modulus E and the shear modulus G which has recognized for many years:

$$G/E \approx 0.356 \quad \ldots\ldots\ldots\ldots\ldots (4)$$

So if we take into account the well-known relation between Young's modulus, the shear modulus and the bulk modulus:

$$G/E = \frac{(3 + G/B)}{9} \quad \ldots\ldots\ldots\ldots\ldots (5)$$

Table (3) below indicate the values of shear modulus, bulk modulus, Poisson's ratio and the parameters (G/E, G/B, E/B and ((3+(G/B))/9) for quenched ribbons, and that is obviously equations (4,5) are almost satisfied.

Table 3: young modulus, Shear modulus, bulk modulus, Poisson's ratio and G/E, G/B, E/B, (3+(G/B)/9) values

System	young modulus (Gpa)	Shear modulus (Gpa)	Bulk modulus (GPa)	Poisson's ratio	G/E	G/B	E/B	(3+(G/B))/9
$Pb_{86.9} – Sb_{13.1}$	12.5	4.38	27.9	0.43	0.350	0.156	0.44	0.350
$Pb_{85.9}$ - $Sb_{13.1}$ - Bi_1	13.5	4.74	29.8	0.42	0.351	0.159	0.45	0.351
$Pb_{84.9}$ - $Sb_{13.1}$ - Bi_2	15.5	5.44	33.7	0.42	0.351	0.161	0.45	0.351
$Pb_{83.9}$ - $Sb_{13.1}$ - Bi_3	16.1	5.67	34.6	0.42	0.351	0.163	0.46	0.351
$Pb_{82.9}$ - $Sb_{13.1}$- Bi_4	17.3	6.09	36.6	0.42	0.351	0.166	0.47	0.351
$Pb_{81.9}$ - $Sb_{13.1}$ - Bi_5	10.5	3.69	21.9	0.42	0.352	0.168	0.47	0.352

The microhardness of eutectic alloy was also increase with increasing of bismuth content. Microhardness of the original Pb – Sb eutectic alloy was 130.34 (Mpa).An addition of Bi at 4 wt. % to eutectic alloy the microhardness increase to 187.768 (Mpa). This indicates the powerful effect of bismuth in improving Young's modulus and microhardness of binary eutectic system. The increasing of Young modulus and microhardness of this alloy can be explained by microstructure

ISSN 2347-3487

analysis of the alloy. Figure (5) show that both of microhardness with bismuth content. As we see from table (4) hardness of Pb–Sb–Bi melts spun alloys.

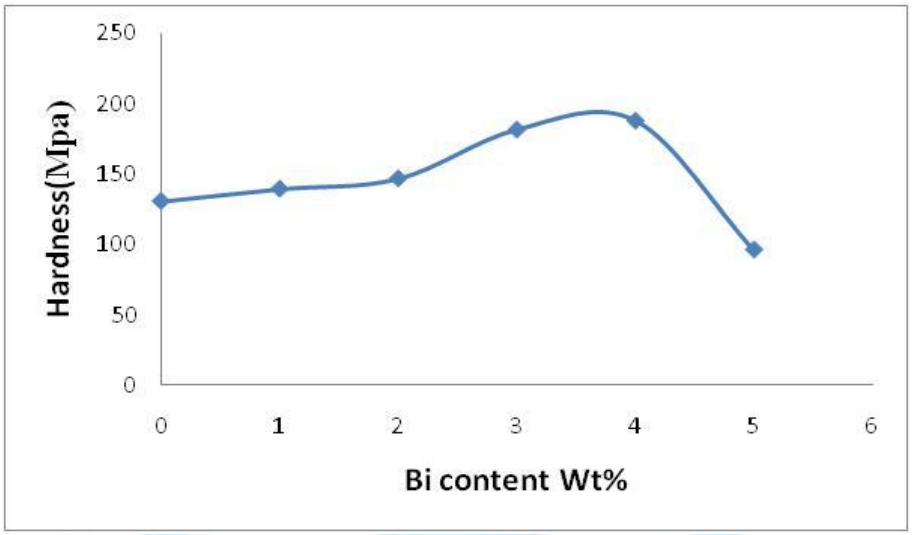

Fig. (5): Microhardness Vs. Bi content

Table 4: Hardness of Pb – Sb – Bi melt spun alloys

system wt%	Hardness(Mpa)
$Pb_{86.9}$ - $Sb_{13.1}$	130.340
$Pb_{85.9}$ - $Sb_{13.1}$ - Bi_1	139.160
$Pb_{84.9}$ - $Sb_{13.1}$ - Bi_2	146.510
$Pb_{83.9}$ - $Sb_{13.1}$ - Bi_3	181.398
$Pb_{82.9}$ - $Sb_{13.1}$ - Bi_4	187.768
$Pb_{81.9}$ - $Sb_{13.1}$ - Bi_5	95.648

Another important characteristic of melt-spun ribbons can be calculated from frequency f_o, at which peak damping occurs which is internal friction (Q^{-1}). Internal friction measurements have been quite fruitful for learning the behavior of rapidly quenched ribbons from melt. It is one of the important characteristics which are indirectly related to their elastic properties. The free vibration is based on the measurement of the decay in amplitude of vibrations during free vibration. The internal friction is obtained by:

$$Q^{-1} = 0.5773\left(\frac{\Delta f}{f_o}\right) \quad \ldots\ldots\ldots\ldots (6)$$

From table (5) we can see internal friction decreased after adding bismuth content.

Table 5: f (Hz), FWHM (Hz) and internal friction

system wt%	f_o (Hz)	Δf (Hz)	$Q^{-1}\times10^{-3}$
$Pb_{86.9}$ - $Sb_{13.1}$	13.60	1.74	74
$Pb_{85.9}$ - $Sb_{13.1}$ - Bi_1	23.16	0.55	13
$Pb_{84.9}$ - $Sb_{13.1}$ - Bi_2	20.17	0.59	17
$Pb_{83.9}$ - $Sb_{13.1}$ - Bi_3	26.20	0.61	13

$Pb_{82.9}$ - $Sb_{13.1}$ - Bi_4	13.14	0.98	43
$Pb_{81.9}$ - $Sb_{13.1}$ - Bi_5	11.71	1.162	57

3.5 Electrical properties.

The rate of rise of electrical resistivity of a metal with temperature is dependent on the small amount of alloying present and on the state of deformation. The actual cause of resistivity must therefore be sought in deviations from the periodicity of the potential in which the electron move. It is on this concept that the modern theory of conductivity is based. Deviations from the periodicity of the potential causing resistivity maybe due to: (1) boundaries (2) lattice defects (3) lattice vibrations (4) foreign impurity atoms. Table 6 shows the room temperature resistivity (ρ_o) of the Pb-13.1Sb-Bix(X= 0, 1,2,3,4 and 5) melt spun alloys. It shows that, the resistivity of the eutectic alloy is equal to 7.92×10^{-7} Ω.m. All Bi additions to this alloy increase this value except the case of Bi at 4 wt.% that slightly decreases to 7.49×10^{-7} Ω.m. This decrease can be attributed to precipitation of Bi phase, which has lower value of resistivity than that of Sn-matrix. While, the higher values can be attributed to the formation of the Sb phase which act as scattering centers for conduction electrons.

Table 6: Electrical properties and Lorenz number of all melt spun alloys

system wt%	Resistivity $(\Omega.m)*10^{-7}$	Conductivity $(\Omega^{-1}.m^{-1})*10^{6}$	Thermal Conductivity $K(\Omega^{-1}.m^{-1}.\circ k)$	Lorenz number $*10^{-9}$
$Pb_{86.9}$ - $Sb_{13.1}$	7.92	1.26	1.91	5.1
$Pb_{85.9}$ - $Sb_{13.1}$ - Bi_1	12.5	0.799	1.22	5.1
$Pb_{84.9}$ - $Sb_{13.1}$ - Bi_2	10.2	0.977	1.48	5.1
$Pb_{83.9}$ - $Sb_{13.1}$ - Bi_3	12.2	0.817	1.24	5.1
$Pb_{82.9}$ - $Sb_{13.1}$ - Bi_4	7.49	1.33	2.01	5.1
$Pb_{81.9}$ - $Sb_{13.1}$ - Bi_5	9.24	1.08	1.64	5.1

From table (6) we can see decreasing in thermal conductivity after adding bismuth content except exist increased when added (4 wt%) from bismuth content.

Conclusions

From previous results it can be concluded the following:

In this paper, the increase of Bi content to Pb-Sb bearing-solder alloy was proved to be an effective way to improve the microstructure and properties.

a) It is apparent from our experience there is a great benefit to be used melt-spinning technique, which have proved to be a powerful techniques in numerous commercial melt-spun ribbon alloy systems.

b) In terms of electrical properties, the addition of bismuth increase the resistance except for addition (4 wt%) where the lowest value of the resistance about 7.49×10^{-7} Ω.m.

c) In terms of mechanical properties, the addition of bismuth to binary eutectic alloy Pb-13.1Sb cause an increase in the Young's modulus and hardness except for the addition (5wt%) it less, This indicates the powerful effect of bismuth in improving Young's modulus and hardness.

d) It is clear decrease in the value of the internal friction after the addition of bismuth content.

e) In terms of thermal properties can be seen that the degree of melting temperature, enthalpy, entropy and specific heat are decreased after the addition of bismuth.

References

[1] N.I.Varich and A.A.Yakumin Russian, J.Phys. Chem. 41, pp. 437-440 (1976).

[2] C.Borromee-Gautier, Bill C.Giessen and N.J.Grant the journal of Chemical Physics, Vol.48, No.5, March, 1905, (1968).

[3] P.Ramachandraro, P.K. Grang and T.R. Anantharaman, Indian Journal of Technology, Vol.8, July, p.263(1970).

[4] M.Kamal, R.M.Shalaby, Journal of Materials Science and Technology, Vol.11, No.4 (2003) pp.58-63.

[5] Z. Jiang, Y. Lu, S. Zhao, W. Gu and Z. Zhang, J. Power Sources 31, 169 (1990).

[6] Diagrammy sostoyaniya dvoinykh metallicheskikh sistem: Spravochnik (Phase Diagrams of Binary Metal Systems:Handbook), vol. 3, book 1, Lyakishev, N.P., Ed., Moscow: Mashinostroenie, 2001].

[7] Hultgren, R., Orr, R., Anderson, P., and Kellsy, K., Selected Values of Thermodynamic Properties of Metals and Alloys, New York–London, 1963, p. 963.

[8] Morachevskii, A.G., Voronin, G.F., Geiderikh, V.A., and Kutsenyuk, I.B., Electrokhimicheskie metody issledovaniya v termodinamike metallicheskikh sistem (Electrochemical Methods of Investigation in Thermodynamics of Metal Systems), Moscow: Akademkniga, 2003.

[9] Oelsen, W., Johannsen, F., and Podgornik, A., Z. Erzbergbau und Metallhütten, 1956, vol. 9, p. 459.

[10] Seltz, H. and De Witt, B.J., J. Amer. Chem. Soc., 1939, vol. 61, p. 2594.

[11] Gul'din, I.T. and Rozlovskii, A.A., Tsvetn. Met. (Moscow), 1972, no. 1, p. 81.]

[12] R.S. Dean, The System Lead-Antimony, J. Am. Chem. Soc.,1923, 45, p 1683-1688

[13] B. Blumenthal, The Constitution of the Lead-Antimony and Lead-Antimony-Silver Systems, Trans. AIME, 1944, 156, p 240-252

[14] Z. Moser, K.L. Komarek, and A. Mikula, Thermodynamics and Phase Diagram of the Lead-Antimony System, Z. Metallkd., 1976, 67, p 303-306

[15] M. Kamal,J.C.Pieri and Jouty, Memories et Etudes Scintifiques Revue de Metalurgie – Mars, P. 143 (1983).

[16] N B. Dahotre. M. H. McCay, T. O. McCay and M. M. Kim, J. Mater. Sci.27, P. 6426(1992)

[17] Mustafa Kamal, Abu-Bakr El-Bediwi and Mohammed .S. Jomaan, International Journal of Modern Applied Physics, 2013, 2(1): 1-14.

[18] Mustafa Kamal, Abu-Baker El-Bediwi and Tarek El-Ashram, Journal of Materials science in Electronics 15(2004) 211-217.

[19] Rizk Mustafa Shalaby and Mustafa Kamal, International Journal of physic and Research (IJPR), Vol.13, Issues, Dec. (2013), 51-60

[20] Mustafa Kamal, Shalabia Badr and Nermin Ali Abdelhakim, International Journal of Engineering and Technology IJET-IJENS Vol: 14, No: 01 Feb. (2014) IJENS, PP: 119-129.

[21] Mustafa Kamal, Abu-Baker El-Bediwi and Jamal Khalil Majeed, International Journal of Engineering and Technology IJET-IJENS Vol.14, No: 02 April (2014) IJENS, PP: 5 -15.

[22] Mustafa Kamal and Abu-Baker El-Bediwi, Radiation Effects and Defects in solids 174(1999)211.

[23] Whetten R.L., Khoury J.T., Alvarez M.M., Murthy S., Vezmar I., Wang Z.L., Stephens P.W., Cleveland C.L., Luedtke W.D.and Landman U., Nanocrystal gold molecules;Advan. Mater; 1994; 8: 428-433.

[24] Murray C.B., Kagan C.R. and Bawendi M.G., Self-Organization of CdSe Nanocrystallites into Three-Dimensional Quantum Dot Superlattices; Scienc; 1995; 270: 1335-1338.

[25] Murray C.B., Kagan C.R. and Bawendi M.G., Synthesis and Characterization of Monodisperse Nanocrystals and Close-Packed Nanocrystal AssembliesAnn. Rev. Mater. Sci.; 2000; 30: 545-610.

[26] B.D.Cullity; Elements of X-ray Diffraction, 2nd Edition,Addison-Wesely Publishing Company ,pp.248,(1978).

[27] R.M. Shalaby, Materials Science & Engineering A 560 (2013) 86–95

[28] B. Huang, N.C. Lee, Int. Symp. Microelectron. Proc. 3906 (1999) 711.

[29] F.Q. Zu, Z. G. Zhu, B. Zhang, Y. Feng and J.P. Shui, J. phys. Condens. Matter 13 (2001) 11435-11442

[30] E. Schreiber, O. L. Anderson, and N. Soga, Elastic Constants and their Measurements, McGraw-Hill Book Company (1973) PP: 82-125.

[31] H. M. Ledbetter, Material Science and Engineering, 27(1977) 133.

[32] T. Gorecki, Material Science and Engineering, 43(1980) 225.